The Effect of Operating Temperatures on Wax Deposition

ARTICLE *in* ENERGY & FUELS · OCTOBER 2011

Impact Factor: 2.79 · DOI: 10.1021/ef201048w

5 AUTHORS, INCLUDING:

Rainer Hoffmann
Linde Group
18 PUBLICATIONS **126** CITATIONS
SEE PROFILE

H. Scott Fogler
University of Michigan
284 PUBLICATIONS **8,176** CITATIONS
SEE PROFILE

energy&fuels

ARTICLE

pubs.acs.org/EF

The Effect of Operating Temperatures on Wax Deposition

Zhenyu Huang,[†] Yingda Lu,[†] Rainer Hoffmann,[‡] Lene Amundsen,[‡] and H. Scott Fogler[†,*]

[†]Department of Chemical Engineering, University of Michigan, Ann Arbor, Michigan 48109, United States

[‡]Herøya Research Centre, Statoil ASA, N-3908 Porsgrunn, Norway

ABSTRACT: In this study, a deposition model called the Michigan Wax Predictor (MWP) was used to establish criteria as to whether the rate of wax deposition increases or decreases as the oil/coolant temperature is changed in a series of flow-loop experiments. The model was able to predict the effects of the temperature conditions on wax deposition without applying any adjustable parameters. Despite the fact that many previous studies have used the "thermal driving force" to characterize the effect of temperature on wax deposition, it was not the most comprehensive predictive parameter, as it neglects the importance of the solubility curve on wax deposition. This study has revealed that the most important factors affecting deposition are the mass driving force and the shape of the solubility curve. The major impact of the shape of the solubility curve is to affect the change in characteristic mass flux for wax deposition the when the oil and the coolant temperatures are changed. In particular, the differences in the shapes of the solubility curve can be used to explain the discrepancies on the effect of the oil temperature on wax deposition observed in different deposition studies.

1. INTRODUCTION

1.A. Background. Wax deposition in subsea pipelines is a major flow assurance problem in the petroleum industry. When crude oil at a high temperature (70−120 °C) from subsea reservoirs flows through the pipelines on the ocean floor (4 °C), the heat loss from the crude oil to the seawater causes wax molecules to deposit on the pipe wall.[1] The deposition poses a significant problem for petroleum transportation by creating flow constrictions that can increase the pressure drop in the pipe and increase the production cost. The deposit can even grow to a point where the pipeline becomes plugged, causing production to be stopped in order to replace the plugged portion of the pipeline.[2] The development and application of the remediation techniques for wax deposition have become a vital part of the flow assurance practice and research. Significant production cost can be attributed to these techniques, include pigging, pipeline insulation, heating, and fused chemical reactions.[3] Using pigging as an example, insufficient pigging frequency can result in a deposit that grows so thick that the pig has been known to get stuck, which stops the flow of petroleum fluids. However, too high of a pigging frequency can lead to additional costs of tens of millions of dollars due to deferred production.[4] To arrive at an optimal pigging frequency, the rate of wax deposition needs to be determined. This rate of deposition is thought to change along the axial direction in a subsea pipeline because of continuous heat losses that are experienced by the crude oil.[5] The loss of heat in the oil causes the variation in the temperature gradient along the pipe, which alters the driving force for wax deposition.[6]

To study the wax deposition in the subsea pipelines, many lab-scale experimental studies have been carried out for different operating temperatures.[7−10] Coldfinger and flow-loop experiments are the two commonly used apparatii. In coldfinger experiments, a small cylindrical metal heat exchanger (the coldfinger) is maintained at a lower temperature and is submerged in a bulk crude oil of a higher temperature. The temperatures of the coldfinger and the bulk crude oil are controlled by two separate water baths. By changing the bulk oil temperature and the coldfinger temperature, the wax deposition can be studied for different thermal gradients.[7,8] Although the coldfinger experiments do provide some insights on wax deposition, they certainly are not a direct representation of wax deposition in field-scale pipelines because of the differences in geometries and flow fields between a coldfinger system and a pipe flow-loop system.[9] The flow-loop apparatus better simulates the conditions for wax deposition in subsea pipelines compared to coldfinger devices. Most flow-loops are equipped with an annular pipe where the crude oil flows in the inner pipe while the coolant flows through the annulus. By changing the temperatures of the oil and the coolant, the thermal conditions at different axial positions of the subsea pipeline can be simulated.[6,9,10] In these studies, the temperature difference between the bulk oil and the coolant (or the coldfinger temperature) is frequently referred to as the "thermal driving force" for wax deposition. A comparison of these studies is discussed to review the wax deposition characteristics for different temperature conditions.

1.B. Decreasing Wax Deposition with Decreasing Thermal Driving Force. Jennings et al. used a coldfinger apparatus and a crude oil from the Gulf of Mexico to study wax deposition at different coldfinger temperatures while the bulk temperature of the oil was kept constant.[7] It was found that the experiments with higher coldfinger temperatures (smaller thermal driving force) yielded smaller amounts of deposit. Creek et al. found similar results using a flow-loop apparatus to study wax deposition for different coolant temperatures.[9] Their study showed that the deposit thickness decreased when the coolant temperature increased (decreasing thermal driving force). In the study by Bidmus et al., four different inlet temperatures were examined while the coolant temperature was kept constant. It was found that a decrease in the oil temperature (decreasing thermal driving force)

Received: July 18, 2011
Revised: September 26, 2011
Published: September 28, 2011

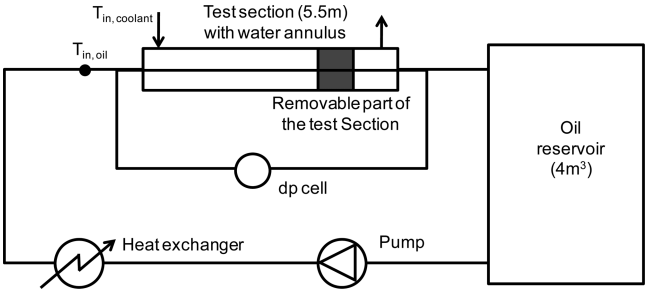

Figure 1. Schematic of the flow-loop experiment for wax deposition.[11]

to near ambient or pipe-wall temperatures could substantially decrease wax deposition. In all the above studies, a generalization was made that the deposit thickness decreases when thermal driving force decreases. In the above studies, the focus on the thermal driving force for wax deposition is based on the fact that molecular diffusion was assumed to be the most prevalent wax deposition mechanism.[6−13] In this mechanism, the mass flux of the wax molecules at the interface (from the oil toward the deposit) $(D_{wo,interface}(dC/dr)|_{interface,fromoil})$ represents the loss of wax from the oil to form a deposit. Among the parameters in the mass flux, the concentration gradient $(dC/dr|_{interface,from\ oil})$ can be approximated by applying the chain rule and using two parameters: the radial temperature gradient, $(\partial T/\partial r|_{interface,from\ oil})$ and the solubility gradient (dC/dT), as shown in eq 1.

$$D_{wo,interface}\left.\frac{dC}{dr}\right|_{interface,from\ oil} \approx D_{wo,interface}\left(\left.\frac{dT}{dr}\right|_{interface,from\ oil}\right)\left(\frac{dC}{dT_{interface,from\ oil}}\right) \quad (1)$$

The first term of the right-hand side (RHS) of eq 1, namely, the radial temperature gradient, has been the focus in previous studies where the thermal driving force has been considered as the major parameter to explain the temperature effects on wax deposition.[7,9,10] However, equally important is the solubility gradient at the oil-deposit interface, that is, the second parameter on the RHS of eq 1, and it is frequently overlooked in theoretical analyses. The solubility gradient reflects the effect of the shape of the solubility curve on wax deposition. For particular types of oil, the impact on the solubility curve can overcome the effect of the temperature gradient when the operating conditions change.

1.C. Increasing Wax Deposition with Decreasing Thermal Driving Force. Coldfinger studies by Paso and Fogler on other oils at lower temperatures showed an opposite trend to that discussed above, where more wax molecules can precipitate and form thicker deposits with decreasing temperature gradients.[8] This trend was attributed to a result of an increase in the wax precipitation at the coldfinger surface, which was not accounted for in any of the previous studies. However, this trend had not been previously observed in flow-loop experiments, until this work.

2. WAX DEPOSITION EXPERIMENTS

In the study reported here, a series of experiments was carried out using a laboratory flow-loop in the Herøya Research Center of Statoil ASA in Porsgrunn, Norway. An oil from the North Sea identified as North Sea oil A is provided by Statoil ASA and was used in this study for deposition experiments. In addition, the experimental results from a previous study by Bidmus et al.,[10]

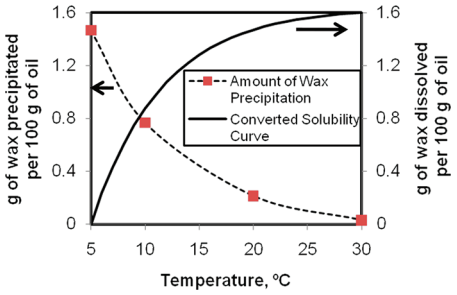

Figure 2. Amount of precipitation of wax in oil at various temperatures and the corresponding solubility curve for the North Sea oil A.

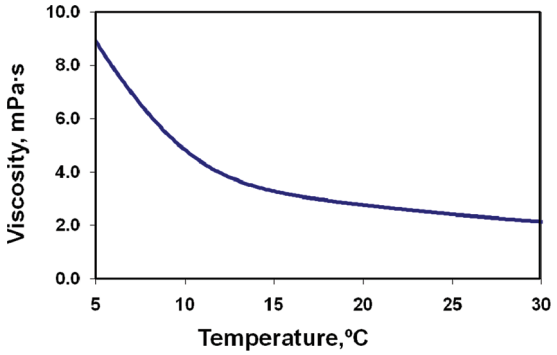

Figure 3. Viscosity of North Sea oil A at different temperatures.

using a model oil−wax system, will be used as a comparison in this study. Because the solubility curve of the model oil used in the study by Bidmus et al. was not provided, it was measured in the current study using differential scanning calorimetry (DSC).

2.A. Flow-Loop Experiments with North Sea Oil A. *2.A.1. Flow-Loop for Wax Deposition Experiments.* A sketch of the flow-loop from the Herøya Research Centre of Statoil ASA is shown in Figure 1. The flow-loop is equipped with a reservoir of 4 m^3 and a test section with a length of 5.5 m and an inner diameter (i.d.) of 5.3 cm. The deposit thickness was calculated from pressure-drop measurements in the test section. The values of the calculated wax thickness were confirmed by laser measurements of the wax in the oil deposit at the end of an experiment. The detailed information of flow-loop, along with the characterization techniques to study wax deposition, has been reported by Hoffmann and Amundsen.[11]

2.A.2. The Solubility and Viscosity−Temperature Curves for North Sea Oil A. The North Sea oil A used for this research has a cloud point of approximately 30 °C. The amount of precipitation of wax in the oil at various temperatures was measured using the centrifugation and gas chromatography techniques, as reported by Han et al. and shown in Figure 2.[12] The solubility curve of the North Sea oil A is an important input parameter for wax deposition modeling. It was obtained by assuming that, in the end, all the wax has precipitated out of the oil at 5 °C. In this case, the total wax content is the same as the precipitation of wax at 5 °C, as shown in Figure 2. Because the coolant temperatures of all the experiments are no less than 5 °C, the wall temperatures of all the experiments are higher than 5 °C. Because the temperature of the wall is the lowest point in the flow-loop system, the amount of wax precipitation in this North Sea oil A below the wall temperature is not needed for model predictions in this study. Similarly, the solubility curve for the model oil is shown for

dx.doi.org/10.1021/ef201048w |*Energy Fuels* 2011, 25, 5180–5188

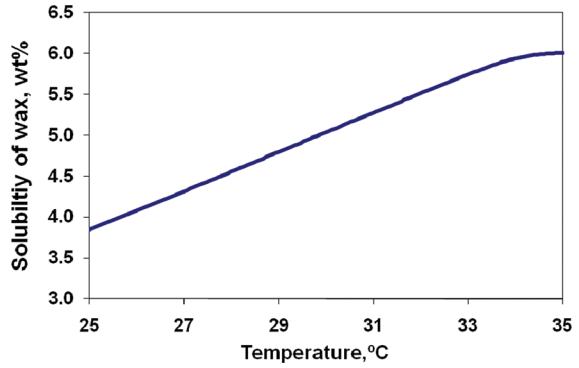

Figure 4. Solubility curve of wax for the model oil.

the temperature above 25 °C in Figure 4, which is the coolant temperature in the corresponding experiments.

In addition, the viscosity of the North Sea oil A was measured as a function of temperature using a Physia MCR 301 Rheometer. The viscosity−temperature curve is shown in Figure 3.

2.B. The Solubility−Temperature Curve of the Model Oil in the Study by Bidmus et al.[10]. A previous study by Bidmus et al. using a model oil with 6% wax content and a cloud point of 35 °C was chosen as the basis of comparison for this research. Most of the properties of this model oil can be found in the work of Bidmus et al.[10] However, the solubility of wax was not reported in their study. To measure this parameter, we purchased the same solvent, Norpar13 from Imperial Oil (Ontario, Canada), and the same wax sample, Parowax from Conros Corp (Ontario, Canada), that were used by Bidmus et al. The solubility was measured with a TA Q2000 DSC. The oil was first heated to 60 °C and held at this temperature for 30 min to remove any thermal history and then cooled from 60 to −40 °C at a rate of 1 °C/min. The solubility curve of the model oil was obtained by assuming that the heat release is proportional to the amount of precipitated wax, as shown in Figure 4.

Comparing Figures 2 and 4, it can be noted that as the oil is cooled, the solubility of the model oil is not as temperature-sensitive as the North Sea oil A.

3. THEORETICAL ANALYSIS USING THE MICHIGAN WAX PREDICTOR (MWP)

3.A. Model Introduction. A mathematical model (the Michigan Wax Predictor (MWP)) based on earlier studies of Singh, Lee, Huang et al. was applied to investigate the temperature effects on wax deposition.[1,6,13] The MWP applies the Graetz boundary conditions, and the flow of the oil is assumed to be in a quasi-steady state, while the wax thickness, δ, increases with time. The external heat transfer coefficient for the coolant was calculated using the correlation by Monrad and Pelton to account for the heat loss to the coolant flowing in the annuli of the pipe.[14] The internal heat and mass transfer rates were calculated using a 2D axial symmetry energy equation and the correlation for eddy diffusivity by Van Driest.[15] The model calculates the axial convection and the radial conduction/diffusion for the heat and mass transfer equations to determine the temperature profile as well as the concentration profile of wax molecules, as shown in Figure 5.

With the information of the concentration profile, the concentration gradient at the interface is thereby determined to

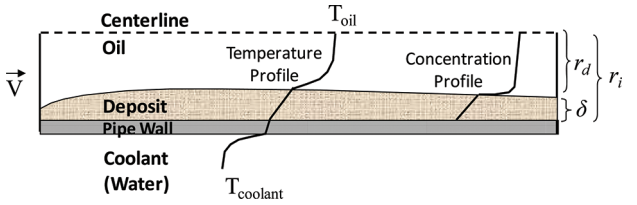

Figure 5. Sketch of the wax deposition mechanism.

calculate the growth rate of both the deposit thickness and the wax fraction in the deposit, using molecular diffusion as the major mechanism for wax deposition. The details of this model can be found in the work of Lee and Huang et al.[1,13]

It should be noted that the equations in the model were developed from first principles and that no tuning parameters were used. In this analysis of mass transfer, it is assumed that wax molecules only precipitate in the deposit and that they do not precipitate in the oil phase. This approach is similar to the one used in the laminar flow model by Singh et al., where the heat and mass transfer correlations were decoupled.[6] In addition, the model in the current study does not need to incorporate the so-called "shear removal" effect, that is, the detachment of the deposited wax material from the pipe wall by the flowing oil, to predict the observed trends. Because the effect of bulk precipitation and shear removal are highly empirical, the use of tuning parameters to include these effects can reduce the reliability for our conclusions. Consequently, the major focus of this model is to examine a number of deposition experiments in general to determine whether the model repeats the trends shown in the experiments rather than comparing each experiment with their corresponding model predictions.

3.B. Determining Parameter for Wax Deposition. To look for a more representative driving force for wax deposition than the thermal driving force, the MWP analyzes the mass balance equation shown in eq 2, along with the boundary conditions shown in eq 3:

$$V\frac{\partial C}{\partial z} = \frac{1}{r}\frac{\partial}{\partial r}\left[(\varepsilon_{\text{mass}} + D_{\text{wo}})r\frac{\partial C}{\partial r}\right] \tag{2}$$

$$\begin{cases} \text{at } z = 0,\ C = C_{\text{inlet}} \\ \text{at } r = 0,\ \dfrac{\partial C}{\partial r} = 0 \\ \text{at } r = r_{\text{d}},\ C = C_{\text{interface}} \end{cases} \tag{3}$$

The following dimensionless ratios given in eq 4 were used to dedimensionalize the mass balance equation and the boundary conditions shown in eqs 2 and 3, resulting in eqs 5 and 6.

$$\left(\theta = \frac{C - C_{\text{interface}}}{C_{\text{inlet}} - C_{\text{interface}}}\right),\ \left(v = \frac{V}{U}\right),\ \left(\lambda = \frac{z}{L}\right),$$
$$\left(\eta = \frac{r}{r_{\text{d}}}\right),\ \left(\text{Gz}_{\text{t}} = \frac{d_{\text{d}}^2 U}{L(\varepsilon_{\text{mass}} + D_{\text{wo}})}\right) \tag{4}$$

$$v\frac{\partial \theta}{\partial \lambda} = \frac{1}{\eta}\frac{\partial}{\partial \eta}\left[\frac{4}{\text{Gz}_{\text{t}}}\eta\frac{\partial \theta}{\partial \eta}\right] \tag{5}$$

$$\begin{cases} \text{at } \lambda = 0,\ \theta = 1 \\ \text{at } \eta = 0,\ \dfrac{\partial\theta}{\partial\eta} = 0 \\ \text{at } \eta = 1,\ \theta = 0 \end{cases} \tag{6}$$

One notes that the solution profile of the de-dimensionalized variable θ, from eqs 5 and 6, is independent of the changes in C_{inlet} and $C_{interface}$. Consequently, the radial mass flux of wax molecules from the bulk toward the interface can be found to be proportional to $[D_{wo,interface}(C_{inlet} - C_{interface})]$, as given by eq 7.

$$D_{wo,interface}\left.\frac{dC}{dr}\right|_{interface} = D_{wo,interface}\frac{\partial C}{\partial\theta}\left(\left.\frac{\partial\theta}{\partial r}\right|_{interface}\right)$$
$$= \frac{D_{wo,interface}(C_{inlet} - C_{interface})}{r_d}\left(\left.\frac{\partial\theta}{\partial\eta}\right|_{interface}\right) \tag{7}$$

The impact of temperature on the concentration differences $(C_{inlet} - C_{interface})$ can be seen by assuming thermodynamic equilibrium for the concentrations, in which case the solubility curve of the oil can be used to obtain a form of mass flux, J, as given in eq 8.

$$J = \frac{D_{wo,interface}(C_{inlet} - C_{interface})}{r_d} \approx \frac{D_{wo,interface}[C_{inlet}(eq) - C_{interface}(eq)]}{r_d} \tag{8}$$

In addition, the effect of the temperature on the diffusivity can be estimated using the Hayduk−Minhas correlation as shown in eq 9.[16]

$$D_{wo,interface} = 13.3 \times 10^{-12}\frac{T_{interface}{}^{1.47}\mu^{(10.2/V_A - 0.791)}}{V_A{}^{0.71}}\ m^2/s \tag{9}$$

Difficulties arise when one tries to evaluate $D_{wo,interface}$ and $C_{interface}(eq)$ because they depend on the interface temperature, $T_{interface}$, which, in turn, greatly depends on the predicted value of an existing deposit thickness. Therefore, one needs to know the exact thickness of the deposit to accurately determine $C_{interface}(eq)$ and $D_{wo,interface}$. This hurdle can be resolved by evaluating the values of $D_{wo,\ interface}$ and $C_{interface}(eq)$ initially (at $t = 0$ and $\delta = 0$), where deposition has not yet occurred. In this case, $C_{interface}(eq)$ simply reduces to $C_{wall}(eq)$, $D_{wo,interface}$ reduces to $D_{wo,wall}$, and r_d reduces to r_i. Because the wall temperature, T_{wall}, can be accurately determined by solving the heat transfer equation in the MWP using well established correlations for the eddy diffusivities,[15] $C_{wall}(eq)$ can be obtained from T_{wall}, knowing the solubility curve of the oil, and $D_{wo,wall}$ can be determined through T_{wall}, using the Hayduk−Minhas correlation.[16] It should be noted that, in most of the lab-scale flow-loop studies, no significant axial variations in the bulk concentration were observed for the parameters as a result of the short length of the pipe. Therefore, $C_{inlet}(eq)$ is referred to as $C_{oil}(eq)$, for subsequent quantitative analyses.

The significance of the above analysis is that the impact of the oil/coolant temperatures on wax deposition can be found by investigating their effect on a parameter that has the unit of a mass flux, as shown in eq 10

$$J_{wax} = \frac{D_{wo,wall}}{r_i}[C_{oil}(eq) - C_{wall}(eq)] \tag{10}$$

Consequently, J_{wax} is referred to as the characteristic mass flux for wax deposition. The difference in the concentrations, $[C_{oil}(eq) - C_{wall}(eq)]$, is referred to as the mass driving force in the comparison of the thermal driving force $(T_{oil} - T_{coolant})$ among several deposition studies.[7,9,10] We will show that this mass driving force is the most dominant parameter to affect the behavior of the characteristic mass flux for wax deposition, J_{wax}, when the oil/coolant temperatures are changed. It was found that the conclusions for J_{wax} at $t = 0$ $(\delta = 0)$ also hold for $t > 0$ $(\delta > 0)$. The details of this verification can be found in the Appendix.

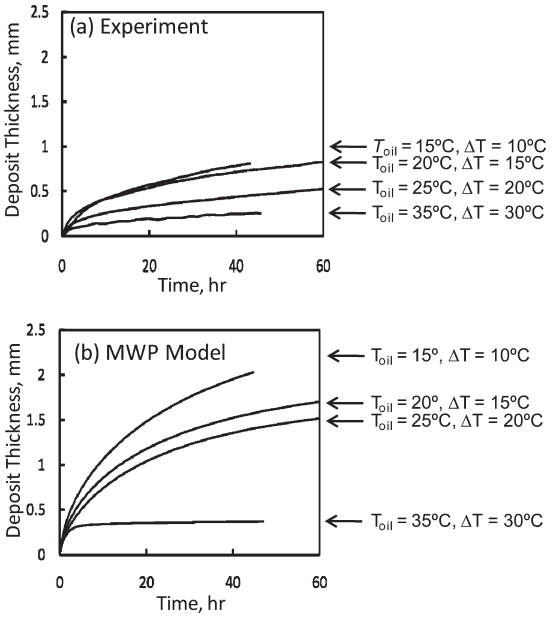

Figure 6. Comparison of deposit thickness as a function of oil temperature, T_{oil}, between (a) the experimental results and (b) the model prediction by the MWP. The oil flow rate, Q_{oil}, was maintained constant at 20 m^3/h, and the coolant temperature, $T_{coolant}$, was maintained constant at 5 °C.

4. RESULTS AND DISCUSSION

4.A. Flow-Loop Results and the Prediction of the Experimental Trends by the Model. Several experimental studies have found that the amount of deposit decreases with decreasing thermal driving force.[7,9,10] However, Figures 6 and 7 show the experimental and theoretical trajectories of wax thickness as a function of time for different operating temperature conditions. The experiments carried out in the current study have shown the two following opposing trends:

Trend 1 (Figure 6): Reduced deposition with increasing oil temperature, T_{oil}, that is, increasing thermal driving force $(T_{oil} - T_{coolant})$.

Trend (2) (Figure 7): Reduced deposition with increasing coolant temperature, $T_{coolant}$, that is, decreasing thermal driving force $(T_{oil} - T_{coolant})$.

These two opposing trends indicate that the thermal driving force is not the best candidate for a theoretical analysis of wax deposition, and other factors exist that better explain the change

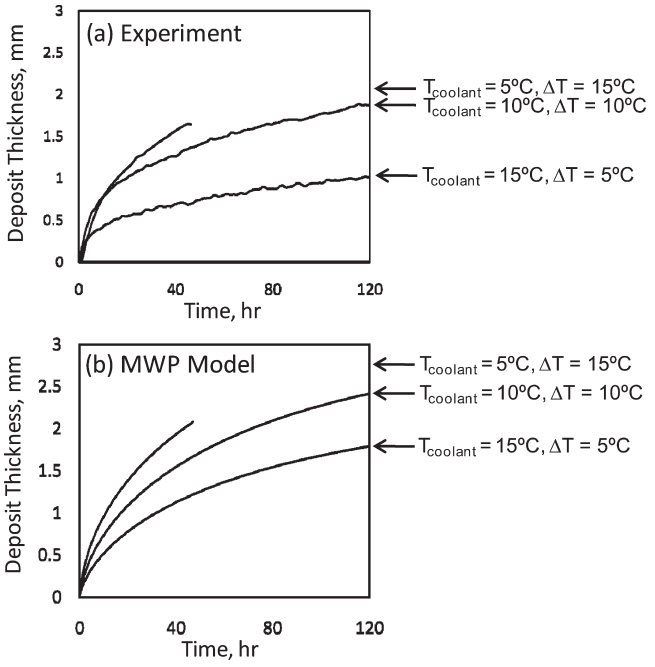

Figure 7. Comparison of deposit thickness as a function of coolant temperature, $T_{coolant}$, between (a) the experimental results and (b) the model prediction by the MWP. The oil flow rate, Q_{oil}, was maintained constant at 5 m^3/h, and the oil temperature, T_{oil}, was maintained constant at 20 °C.

Table 1. Comparison of the Parameters for the Characteristics of Mass Flux for Wax Deposition, J_{wax}, among the Deposition Experiments with Different T_{oil}, while Q_{oil} and $T_{coolant}$ Are Maintained Constant at 5m^3/h and 20°C, Respectively

parameters	values			
Experimental Operating Conditions				
T_{oil}, °C	15.3	20.3	25.3	35.4
$T_{coolant}$, °C	5.0			
Q_{oil}, m^3/h	20.0			
Model Calculations				
T_{wall}, °C	9.5	12.0	14.7	20.5
$D_{wo,wall} \times 10^{10}$, m^2/s	2.11	2.49	2.89	3.64
C_{oil}(eq), wt %	1.09	1.26	1.34	1.43
C_{wall}(eq), wt %	0.65	0.89	1.07	1.26
C_{oil}(eq) − C_{wall}(eq), wt %	0.45	0.36	0.27	0.17
$J_{wax} \times 10^{10}$, m/ s·wt %	36.17	34.14	29.73	23.57

of wax deposition at different oil temperatures. Because of the agreement of the trends between the experiments and the predictions by the MWP, Figures 6 and 7, the MWP will be used to analyze the results shown in this study. In particular, the variations of the parameters in the characteristic mass flux for wax deposition, J_{wax}, for the experiments with different oil/coolant temperatures will be investigated. The parameters consist of the diffusivity, $D_{wo,wall}$, and the mass driving force, $[C_{oil}(eq) - C_{wall}(eq)]$.

4.A.1. Analysis for the Reduced Deposition with Increasing Oil Temperature. Table 1 summarizes the flux term, $\{D_{wo,wall}[C_{oil}(eq) - C_{wall}(eq)]/r_i\}$ and its corresponding parameters for the experiments

Table 2. Comparison of the Parameters for the Characteristic Mass Flux, J_{wax}, among Deposition Experiments with Different Coolant Temperatures, while Q_{oil} and T_{oil} Are Maintained Constant

parameters	values		
Experimental Operating Conditions			
T_{oil}, °C	20.2		
$T_{coolant}$, °C	5.0	10.0	15.0
Q_{oil}, m^3/h	5.0		
Model Calculations (t = 0)			
T_{wall}, °C	8.1	12.1	16.1
$D_{wo,wall} \times 10^{10}$, m^2/s	1.93	2.44	2.97
C_{oil} (eq), wt%	1.26	1.26	1.26
C_{wall} (eq), wt%	0.48	0.89	1.13
C_{oil} (eq) − C_{wall} (eq), wt%	0.78	0.37	0.13
$J_{wax} \times 10^{10}$, m^2/ s·wt%	57.35	34.39	14.71

where the oil temperature, T_{oil}, was varied and the coolant temperature, $T_{coolant}$, was kept constant. In these experiments, the deposition thickness decreased as the oil temperature increases, as shown in Figure 6.

One observes that the increase in T_{oil} leads to an increase in T_{wall}, which affects multiple terms in the characteristic mass flux, $J_{wax} = \{D_{wo,wall}[C_{oil}(eq) - C_{wall}(eq)]/r_i\}$. First, the diffusivity of wax in oil at the wall, $D_{wo,wall}$ increases, which tends to increase the mass flux. Second, the changes in T_{oil} and T_{wall} cause the increases in both $C_{oil}(eq)$ and $C_{wall}(eq)$. Although the change in T_{oil} from 15.3 to 35.4 °C (a change of 20.1 °C) exceeded the change in T_{wall} from 9.5 to 20.5 °C (a change of 11 °C), the change in $C_{oil}(eq)$ from 1.09 to 1.44% (a change of 35%) using the solubility curve was less than the change in $C_{wall}(eq)$ from 0.65 to 1.26% (a change of 61%). Therefore, the mass driving force, $[C_{oil}(eq) - C_{wall}(eq)]$ decreases as the T_{oil} increases and outweighs the increase in $D_{wo,wall}$, resulting in a decrease in the characteristic mass flux, J_{wax}, as can be seen in the last row of Table 1. This decrease in the characteristic mass flux for wax deposition explains the reduced deposit thickness shown in Figure 6 for the experiments with increasing oil temperatures. It should be noted that the difference in the amount of change in the equilibrium concentrations at different temperatures (T_{oil} and T_{wall}) reflects the effect of the concave shape of the solubility curve (Figure 2), where its gradient decreases as temperature increases.

4.A.2. Analysis for the Reduced Deposition with Increasing Coolant Temperature. Now consider the other parameter variation where $T_{coolant}$ was varied and T_{oil} was kept constant. For these operating conditions it was found that the experimental wax thickness decreased as $T_{coolant}$ increased (Figure 7). The characteristic mass flux for wax deposition, $J_{wax} = \{D_{wo,wall}[C_{oil}(eq) - C_{wall}(eq)]/r_i\}$ and its corresponding parameters are shown in Table 2.

It can be seen from Table 2 that the increase in $T_{coolant}$ leads to an increase in T_{wall}, which increased the values of both D_{wo} and $C_{wall}(eq)$. The increase in D_{wo} tends to increase the characteristic mass flux, J_{wax}. However, the increase in $C_{wall}(eq)$ from 0.48 to 1.13% causes a significant decrease in the mass driving force $[C_{oil}(eq) - C_{wall}(eq)]$ from 0.78 to 0.13%. This decrease in the mass driving force overcomes the increase in the diffusivity, leading to a decrease in the characteristic mass flux, J_{wax}, with

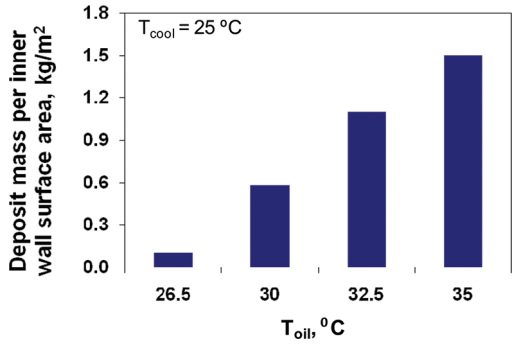

Figure 8. Comparison of the amount of deposit between experiments with different oil temperatures for the study by Bidmus et al.[10]

Table 3. Comparison of the Parameters for the Characteristic Mass Flux, J_{wax} among Deposition Experiments with Different T_{oil} while Q_{oil} and $T_{coolant}$ Are Maintained Constant, from the Study by Bidmus et al., Using a Model Oil

parameters	values			
Experimental Operating Conditions				
T_{oil}, °C	26.5	29.0	33.0	35.0
$T_{coolant}$, °C	25.0			
Q_{oil}, m^3/h	0.4			
Model Calculations				
T_{wall}, °C	25.4	25.9	27.1	28.0
$D_{wo,wall} \times 10^{10}$, m^2/s	2.81	2.94	3.27	3.53
$C_{oil}(eq)$, wt %	4.19	4.80	5.74	6.00
$C_{wall}(eq)$, wt %	3.94	4.05	4.34	4.55
$C_{oil}(eq) - C_{wall}(eq)$, wt %	0.25	0.75	1.40	1.45
$J_{wax} \times 10^{10}$, $m^2/s \cdot wt\ \%$	27.66	86.81	180.24	201.52

increasing $T_{coolant}$, as is shown in the last row of Table 2. This decrease in J_{wax} explains the reduced experimental deposit thickness, as shown in Figure 7.

4.A.3. Analysis of Previous Studies. The increase or decrease in the amount of wax deposit with the change in the temperature conditions can be attributed to the shape of the solubility curve, which causes the equilibrium concentration to behave differently in the bulk oil than at the wall. To further verify this result, the previous study on wax deposition by Bidmus et al.[10] was analyzed. Figure 8 shows the experimental trends from the study by Bidmus et al. from a flow loop with a test section of 2.54 cm i.d. and 10.16 cm length.[10] It can be seen that as T_{oil} increases, the amount of deposit increases, which initially appears to be contradictory to the trend in our study, as shown in Figure 6. However, when we apply the analysis on the characteristic mass flux for wax deposition, J_{wax}, the results are entirely consistent.

The parameters for the mass flux were calculated and shown in Table 3 on the basis of the geometry of the flow-loop and the operating conditions reported in their study.

It can be seen that the increase of T_{oil} from 26.5 to 35 °C had two effects on increasing the mass flux. First, an increase in D_{wo} was observed, which tends to increase J_{wax}. Second, both $C_{oil}(eq)$ and $C_{wall}(eq)$ increased as a result of increased T_{oil} and T_{wall}. More importantly, the increase in C_{oil} from 4.19 to 6.00% is

Table 4. Comparison of the Changes in T_{oil}, T_{wall}, $C_{oil}(eq)$, and $C_{wall}(eq)$ for the Experiments with Both the North Sea Oil A and the Model Oil, where T_{oil} Was Varied[a]

	North Sea oil A	model oil
change in T_{oil}, °C	15.3 − 35.4	26.5 − 35.0
ΔT_{oil}, °C	20.1	8.5
ΔT_{wall}, °C	11.0	2.6
$\Delta T_{oil} > \Delta T_{wall}$	yes	yes
$\Delta C_{oil}(eq)$, wt %	0.35	1.81
$\Delta C_{wall}(eq)$, wt %	0.61	0.61
$\Delta C_{oil}(eq) > \Delta C_{wall}(eq)$	no	yes

[a] The numbers are calculated from Tables 1 and 3.

greater than the increase in C_{wall} from 3.94 to 4.55%, which results in the increase in the mass driving force, $[C_{oil}(eq) - C_{wall}(eq)]$. The combination of the increases in the diffusivity and in the mass driving force results in an increase in the mass flux with increasing T_{oil}, which explains the experimental trends observed in Figure 8, where the amount of deposition increases with increasing T_{oil}.

The importance in the solubility curve to affect the driving force for wax deposition can be seen by comparing the experiments in this study (Figure 6 and Table 1) and those in the study by Bidmus et al. (Figure 8 and Table 3).[10] The changes in T_{oil}, T_{wall}, $C_{oil}(eq)$, and $C_{wall}(eq)$ for the two studies where T_{oil} was varied are shown in Table 4.

One finds that, for both sets of the experiments, the increase in T_{oil} has caused the increase in T_{wall}. The changes in T_{wall} were less significant than those in T_{oil} for both studies. The major difference is that, for the model oil, the gradient of its solubility curve (Figure 4) is virtually constant (i.e., the solubility curve is close to a straight line), so that the changes in $C_{oil}(eq)$ and $C_{wall}(eq)$ simply reflected the changes in T_{oil} and T_{wall}. These changes eventually lead to an increase in the mass driving force, $[C_{oil}(eq) - C_{wall}(eq)]$, and the mass flux, $\{D_{wo,wall}[C_{oil}(eq) - C_{wall}(eq)]/r_i\}$, for the model oil when T_{oil} increased. However, the gradient of the solubility curve for the North Sea oil A decreased with increasing temperature (a concave solubility curve, as shown in Figure 2), resulting in the changes in $C_{oil}(eq)$ and $C_{wall}(eq)$ to deviate from those from in T_{oil} and T_{wall}. Eventually, the change in $C_{wall}(eq)$ outweighs that in $C_{oil}(eq)$, thereby resulting in the increase of the driving force for the North Sea oil A. This finding further demonstrates the advantage of using the mass driving force in comparison to the thermal driving force, as it includes the impact of the solubility curve on wax deposition.

4.B. Comparison between the Carbon Number Distribution of the Model Oil and the North Sea Oil A. The above comparison has highlighted the importance of the shape of the solubility curve on the effects of the oil/coolant temperatures on wax deposition. The solubility of wax represents the multicomponent solid−liquid equilibrium of the oil, which strongly depends on its carbon number distribution. Figure 9a shows the carbon number distributions of the C20+ components in the model oil used in Bidmus et al.,[10] while Figure 9b shows the distribution for the North Sea oil A used in this study. Two major differences can be observed between these two oils. First, a longer tail can be seen in the carbon number distribution of North Sea oil A, indicating the existence of heavy

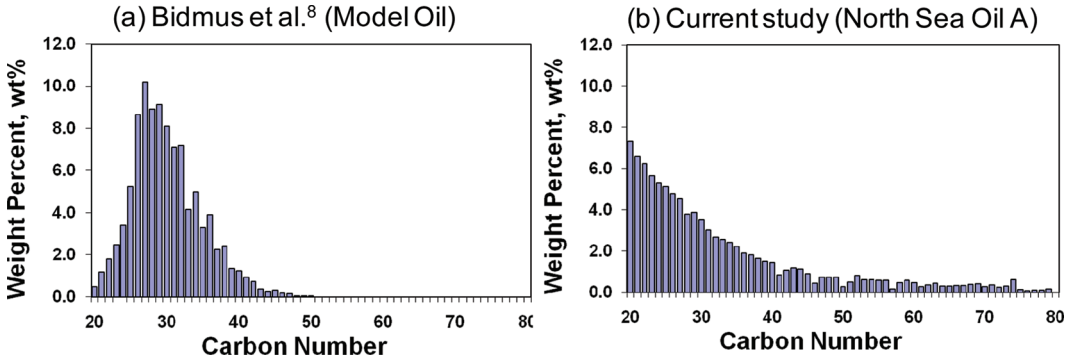

Figure 9. Carbon number distribution of the heavy components in (a) the model oil and (b) the North Sea oil A.

paraffins (C50−C80), which are not existent in the model oil. In addition, lighter components (C20−C26) account for 41% of the wax in North Sea oil A, while they only account for 26% of the wax in the model oil. The small amount of the heavy components and the excess amount of the light components in North Sea oil A causes a greater precipitation of wax at lower temperatures, as compared to the model oil. This greater precipitation is consistent with the concave shape of the solubility curve of the North Sea oil A at low temperatures and eventually explains the contradictory observed trends of growth of deposit thickness between Figures 6 and 8.

4.C. Method to Determine the Effect of Oil/Coolant Temperatures. Based on the analysis above, we have summarized the algorithm to identify the change of the amount of wax deposition with changes in the oil/coolant temperatures as follows:

Step 1. Calculate the wall temperature at the beginning of the experiment, where no wax deposit has yet formed on the wall. This can be done either by solving the heat transfer equation numerically or via the correlations that account for the heat transfer coefficients for the oil and the coolant.[14,15]

Step 2. Calculate the diffusivity of the wax in oil at the wall temperature, $D_{wo,wall}$.

Step 3. On the basis of the solubility curve of the oil, calculate the equilibrium concentrations in the bulk and at the wall, $C_{oil}(eq)$ and $C_{wall}(eq)$, and thus calculate the mass driving force $[C_{oil}(eq) - C_{wall}(eq)]$.

Step 4. Calculate the characteristic mass flux for wax deposition, J_{wax}, as shown in eq 10. Compare this parameter for experiments where the oil or the coolant temperatures are varied. The experiments with a higher mass driving force should have a greater increase in the rate of deposit thickness.

5. CONCLUSIONS

In this study, an analysis was carried out using the Michigan Wax Predictor (MWP) to establish guidelines to determine the effect of the oil and the coolant temperatures on wax deposition thickness. The MWP was first applied to a series of flow-loop deposition experiments, in which the oil temperature and the coolant temperature were all changed independently. It is found that the MWP has successfully predicted the effects of the operating conditions on wax deposition for North Sea oil A without using any adjustable parameters. These effects include reduced deposition with increasing oil temperature and with increasing coolant temperature.

In the subsequent analysis using the MWP, the effect of the oil/coolant temperatures on wax deposition is seen in their impact on the characteristic mass flux for wax deposition, J_{wax}, which includes the diffusivity, $D_{wo,wall}$, and the mass driving force, $[C_{oil}(eq) - C_{wall}(eq)]$. The mass driving force for wax deposition is a more appropriate parameter to quantify the temperature effects on wax deposition in comparison to the thermal driving force $[\Delta T = (T_{oil} - T_{coolant})]$.[7,9,10]

It is found that the shape of the solubility curve can greatly affect the mass driving force by affecting the equilibrium concentrations of wax in the bulk oil and at the wall. The analysis is carried out by investigating the contradictory change in the deposit thickness between experiments using a North Sea oil A and those using a model oil−wax solution. It was found that, for the North Sea oil A, the amount of wax deposit decreases when the oil temperature increases, which is a trend that has not been observed in the study of the model oil−wax solution. By analyzing the parameters involved with the mass flux, $\{D_{wo,wall}[C_{oil}(eq) - C_{wall}(eq)]/r_i\}$, it is found that the difference in the shape of the solubility curves between these two oils can be used to explain the difference in their experimental trends. The concave shape of the solubility curve of the North Sea oil A results in a more drastic change in $C_{wall}(eq)$ compared to $C_{oil}(eq)$, while the linear shape of the solubility curve for the model oil−wax solution leads to a less significant change in $C_{wall}(eq)$ in comparison to $C_{oil}(eq)$. This difference in the changes in the equilibrium concentrations leads to the difference in the behavior of the mass driving force, which eventually explains the opposing trends in the amount of wax deposit observed in the their experiments when the oil temperature is varied. Furthermore, this discrepancy in these two oils' solubility curves is a result of the difference in their carbon number distributions. It should be noted that using model oils in the investigation of wax deposition can lead to significantly different conclusions from those seen in the real crude oils.

■ APPENDIX: CALCULATIONS OF THE CHARACTERISTIC MASS FLUX FOR WAX DEPOSITION AT $\Delta > 0$

The calculations for the parameters for the characteristic mass flux, J_{wax}, at $t = 0$ ($\delta = 0$) are previously shown in Table 1 (for experiments with different T_{oil}) and Table 2 (for experiments with different $T_{coolant}$). To validate that the J_{wax} follows the same trend with respect to the changes in T_{oil} and $T_{coolant}$ for a given thickness of the deposit, Table A1 and Table A2 list the parameters of J_{wax} at $\delta > 0$.

Table A1. Comparison of the Parameters for the Characteristics Mass Flux for Wax Deposition, J_{wax}, among the Deposition Experiments when δ = 0.34 mm with Different T_{oil}, while Q_{oil} and $T_{coolant}$ Are Maintained Constant at 5 m^3/h and 20 °C, Respectively

parameters	values			
Experimental Operating Conditions				
T_{oil}, °C	15.3	20.3	25.3	35.4
$T_{coolant}$, °C	5.0			
Q_{oil}, m^3/h	20.0			
Model Calculations				
t, h	1.32	1.94	2.55	10.39
T_{wall}, °C	12.98	17.10	21.23	29.74
$D_{wo,wall} \times 10^{10}$, m^2/s	2.55	3.14	3.63	4.31
C_{oil}(eq), wt %	1.09	1.26	1.34	1.433
C_{wall}(eq), wt %	0.96	0.17	1.28	1.428
C_{oil}(eq) − C_{wall}(eq), wt %	0.14	0.09	0.06	0.005
J_{wax} (δ = 0.34 mm) × 10^{10}, m/ s·wt %	13.58	10.73	8.61	0.76

Table A2. Comparison of the Parameters for the Characteristic Mass Flux for Wax Deposition, J_{wax}, among the Deposition Experiments when δ = 1 mm with Different $T_{coolant}$ Temperatures, while Q_{oil} and T_{oil} Are Maintained Constant

parameters	values		
Experimental Operating Conditions			
T_{oil}, °C	20.2		
$T_{coolant}$, °C	5.0	10.0	15.0
Q_{oil}, m^3/h	5.0		
Model Calculations			
t, h	11.57	18.62	32.88
T_{wall}, °C	16.30	17.61	18.91
$D_{wo,wall} \times 10^{10}$, m^2/s	3.01	3.18	3.35
C_{oil}(eq), wt %	1.26	1.26	1.26
C_{wall}(eq), wt %	1.14	1.19	1.23
C_{oil}(eq) − C_{wall}(eq), wt %	0.12	0.07	0.03
J_{wax} (δ = 0.34 mm) × 10^{10}, m^2/ s·wt %	14.02	8.68	4.02

It can be seen that the conclusion that J_{wax} increases with increasing T_{oil} and with increasing $T_{coolant}$ is valid for $\delta > 0$.

AUTHOR INFORMATION

Corresponding Author

*Telephone: (734) 763-1361. Fax: (734) 763-0459. E-mail: sfogler@umich.edu.

ACKNOWLEDGMENT

The authors acknowledge the discussions with Oluwasegun Adegoke and Sheng Zheng from the University of Michigan and with Tao Du from the Chinese University of Petroleum. In addition, the authors acknowledge the financial support from the following members of the University of Michigan Industrial Affiliates Program: Chevron, ConocoPhillips, MSi Kenny, Nalco, Shell, Schlumberger, Statoil, and Total.

NOMENCLATURE

Variables

Q = volumetric flow rate (m^3/h).
C = concentration of wax in the oil (wt %).
C(eq) = equilibrium concentration of wax in the oil (wt %).
D_{wo} = mass diffusion coefficient of wax in oil (m^2/s).
$D_{wo}(dC/dr)|_{from\ oil\ to\ interface}$ = Mass flux of wax molecules from the bulk oil toward the oil−deposit interface (m/s) evaluated at the oil−deposit interface.
L = length of the pipe (m).
J = mass flux of wax, kg/m^2·s^{-1}.
J_{wax} = characteristic mass flux for wax deposition, kg/m^2·s^{-1}.
T = temperature (°C).
R = radial coordinate (m).
r_i = radius of the inner pipe (m).
r_d = effective radius of the deposit (m).
t = time (s).
U = averaged velocity of oil (m/s).
Z = axial coordinate (m).
Gz_t = a form of the Graetz number in turbulent flow.

Greek Letters

ε_{mass} = eddy diffusivity for mass (m^2/s).
δ = deposit thickness (m).
Λ = dedimensionalized axial coordinate.
H = dedimensionalized radial coordinate.
ρ = density (kg/m^3).
μ = viscosity (Pa·s).

Subscripts

coolant = properties of the coolant.
inlet = properties of the oil inlet of the pipe.
interface = properties of the oil−deposit interface.
oil = properties of the bulk oil.
wall = properties at the wall.

REFERENCES

(1) Huang, Z.; Lee, H. S.; Senra, M, Fogler, H. S. A Fundamental Model of Wax Deposition in Subsea Oil Pipelines. *AIChE J.* **2011**, *57*, 2955−2964.

(2) Gluyas, J. G.; Hichens, H. M. United Kingdom Oil and Gas Fields. Commemorative Millennium Volume. *Geol. Soc.* **2003**, *20*, 327–333.

(3) Nguyen, D. A.; De Moraes, F. F.; Fogler, S. H. Fused Chemical Reactions. 3. Controlled Release of a Catalyst to Control the Temperature Profile in Tubular Reactors. *Ind. Eng. Chem. Res.* **2004**, *43*, 5862–5873.

(4) Niesen, V. G. The Real Cost of Subsea Pigging. *E&P Mag.* **2002**; Available online: http://www.epmag.com/archives/features/3332.htm.

(5) Alyeska Pipeline Service Company. Low Flow Study−Final Report, June 2011; Available online: http://www.alyeska-pipe.com/Inthenews/LowFlow/LoFIS_Summary_Report_P6%2027_FullReport.pdf

(6) Singh, P.; Venkatesan, R.; Fogler, H. S. Formation and Aging of Incipient Thin Film Wax−Oil Gels. *AIChE J.* **2000**, *46* (5), 1059–1074.

(7) Jennings, D. W.; Weispfennig, K. Effects of Shear and Temperature on Wax Deposition: Coldfinger Investigation with a Gulf of Mexico Crude Oil. *Energy Fuels* **2005**, *19*, 1376–1386.

(8) Paso, K; Fogler, H. S. Bulk Stabilization in Wax Deposition Systems. *Energy Fuels* **2004**, *18*, 1005–1013.

(9) Creek, J. L.; Lund, H. J.; Brill, J. P.; Volk, M. Wax Deposition in Single Phase Flow. *Fluid Phase Equilib.* **1999**, *158*, 801–811.

(10) Bidmus, H. O.; Mehrotra, A. K. Solids Deposition during "Cold Flow" of Wax−Solvent Mixtures in a Flow-loop Apparatus with Heat Transfer. *Energy Fuels* **2009**, *23*, 3184–3194.

(11) Hoffmann, R.; Amundsen, L. Single-Phase Wax Deposition Experiments. *Energy Fuels* **2010**, *24*, 1069–1080.
(12) Han, S.; Huang, Z.; Senra, M.; Hoffmann, R.; Fogler, H. S. *Energy Fuels* **2010**, *24*, 1753–1761.
(13) Lee, H. S. Computational and Rheological Study of Wax Deposition and Gelation in Subsea Pipelines. PhD Thesis, University of Michigan, Ann Arbor 2007
(14) Monrad, C. C.; Pelton, J. G. Heat Transfer by Convection in Annular Spaces. *Trans. AIChE* **1942**, *38*, 593–611.
(15) Van Driest, E. R. On Turbulent Flow Near Wall. *J. Aeronaut. Sci.* **1956**, *23*, 1007–1011.
(16) Hayduk, W.; Minhas, B. S. Correlations for Prediction of Molecular Diffusivities in Liquids. *Can. J. Chem. Eng.* **1982**, *60*, 295–299.